Revista Brasileira de Física, Vol. 16, nº 2, 1986

Surface Electrons on Helium Films*

NELSON STUDART+

Departamento de Fisica, Universidade Federal de São Carlos, Caixa Postal 676, São Carlos, 13560, SP, Brasil

and

OSCAR HIPÓLITO+

Departamento de Física e Ciências dos Materiais, Instituto de Física e Química de São Carlos, USP, Caixa Postal 369, São Carlos 13560, SP, Brasil

Recebido em 29 de julho de 1985; 2ª versão em 22 de novembro de 1985

Abstract Theoretical calculations of some properties of two-dimensional electrons on a liquid helium film adsorbed on a solid substrate are reviewed here. We describe the spectrum of electron bound states on bulk helium as well on helium filrns. The correlational properties, such as the structure factor and correlation energy, are determined asfunctions of the film thickness for different types of substrates in the framework of a Generalized Random-Phase Approximation. The collective excitations of this system are also described. The results for electrons on the surface of thin films and bulk helium are easily obtained. We examine the electron interaction with the excitations of the liquid helium surface resulting in a new polaron state, which was observed very recently. The ground state energy and the effective mass of this polaron are determined by using the path-integral formalism and unitary-transformation method. Recent speculations about the phase diagram of electrons on the helium film are also discussed.

1. INTRODUCTION

The extensive study of the properties of the system formed by electrons on the surface of liquid helium began in the early seventies with the theoretical prediction made by Cole and Cohen[1], and independently by Shikin[2], about the possibility of electrons being trapped on a dieletric substrate where they could be confined by a potential well in the z-direction and could move more or less freely in the X-Y plane of the surface. After this prediction, a series of experiments were performed to investigate this system until Grimes and Brown[3] conclusively observed the existence of these electronic surface states in a beautiful spectroscopic experiment, This experiment consists in the measurement of the microwave absorption as a function of an alternating electric

* This is an invited review article

+ CNPq Research Fellow

field applied in the direction perpendicular to the layer of electrons on the surface of liquid helium. They measured the splittings due to transitions between different electronic states in the potential well by observing the wave absorption as the splittings were tuned into resonance with the frequency of the incident radiation. The motivation for studying this system froma fundamental point of view is that an immense variety of well-defined and clean experiments can be done, which are important for theoretical progress in areas such as phase-transitions in two dimensions, many-body theory, the polaron state, transport phenomena, the Wigner crystallization, etc. Furthermore, realizable techniques of measuring the mobility of surface electrons were employed for studying the thermal surface excitations of quantum liquids and solids. We would like to emphasize the pedagogical appeal of this electronic system. For example, the image-potential-induced surface states are obtained from a very simple one-dimensional Schrödinger equation. Moreover, a large amount of theoretical and experimental work could be done using techniques sucessfully applied to other systems and there are excellent reviews devoted to this field[4-9].

In this paper, we would like to surnmarize some recent theoretical work, emphasizing the case of electrons on the surface of liquid helium adsorved on a substrate.

Theoutlineof this paper isas follows. In section 2, we briefly discuss the general properties of surface electrons on bulk helium, such as the spectrum of bound states, evaluated througli model calculations and compared to the experimental results. The dielectric formulation of this two-dimensional (2D) many-electron system is described and we emphasize the breakdown of the Random-Phase Approximation (RPA) by treating the correlations of the 2D classical plasma. In Section 3, we analyse the new experimental situation with the electrons on the surface of a liquid helium film wetting a solid substrate, We present the change in the spectrum of the electronic states due to film and substrate, By varying the film thickness and taking different substrates one modifies significantly the nature of the electron interaction, from a strictly dipolar potential to the usual Coulomb interaction for electrons confined in a plane. In section 4, we analyse in

detail the influence of the film thickness and several kinds of substrates on the many-body properties of the system, by using a kind of Generalized RPA, the self-consistent field method[10]. We obtain the correlational properties for electrons on the surface o thin films ãnd bulk helium. In section 5, we investigate the self-localization of an electron in a polaronic state by considering its interaction with a cloud of ripplons, the quantum excitations of the helium surface. Our calculations are carried out in the framework of Feynman's path integral formalism[11] as well as in the modified variational scheme of the Lee, Low and Pines theory[12,13]. We discuss the intriguing transition in which the electronic state transforms from a nearly free to a localized state, with a dramatic increase of the effective mass. This polaron transition has been observed quite recently in the electron system levitating above a helium film[14]. And, finally, we describe some recent speculations about the shape of the phase diagram for electrons on helium films, with the possibility of creating a new 20 fluid witk an interesting quantum Wigner transition not yet well studied.

2. SOME PROPERTIES OF THE SURFACE ELECTRONS

The electronic surface states are induced by the interaction potential between the electron and the helium surface, which arises from two different contributions: (i) a long-range interaction coming from the polarization of the liquid surface and given by an attractive image potential and, (ii) a potential barrier due to Pauli's exclusion principle which does not allow an extra electron in the helium atom. The model potential can be constructed as

$$V(z) = \begin{cases} -Qe^2/z & z > 0 \\ V_0 & z \leq 0 \end{cases} \qquad (2.1)$$

$$Q = (1/4)\left[(\varepsilon-1)/(\varepsilon+1)\right] ,$$

where the dielectric occupies the half-space $z < 0$. For helium, we have $\varepsilon \approx 1.057$ and $V_0 = 1$ eV. If one assumes that the barriercanbe approximately taken as infinite and the perpendicular and parallel motions can

be separated, the Schrödinger equation

$$-\frac{\hbar^2}{2m}\nabla^2\Psi_{n,k}(\vec{r},z) + V(z)\Psi_{n,k}(\vec{r},z) = E_{n,k}\,\Psi_{n,k}(\vec{r},z) \qquad (2.2)$$

where

$$\Psi_{n,k}(\vec{r},z) = A^{-1/2}\, e^{i\vec{k}.\vec{r}}\, \Phi_n(z)$$

is solved exactly with the boundary conditions $\Phi_n(0) = \Phi_n(\infty) = 0$. The solutions of the unidimensional (z-direction) Schrödinger equation are given by

$$\Phi_n(z) = z\, R_{n,0}(z) \qquad (2.3)$$

where $R_{n,0}(z)$ are the wavefunctions of the radial equation of the hydrogen atom with zero angular momentum. The energy spectrum is then the well-known spectrum of the hydrogen atom,

$$E_{n,k} = \frac{\hbar^2 k^2}{2m} + \varepsilon_n$$
$$\varepsilon_n = -\frac{Q^2 me^4}{2\hbar^2}\,\frac{1}{n^2} \qquad (2.4)$$

For the lowest subband, one has

$$\Phi_1 = \frac{2}{a_0^{3/2}}\, z\, e^{-z/a_0}, \quad a_0 = \hbar^2/mQe^2 \qquad (2.5)$$

where a_0 is the effective Bohr radius and $\varepsilon_1 = 7\times10^{-4}$ eV for electrons on helium.

Spectroscopic measurements by Grimes *et al.*[15] showed that the transitions between the ground state and the first excited states are about 5% larger than those predicted by the hydrogenic model given by eq. (2.4), as shown in the table below

Transition	Theory	Experiment
1 — 2	119.7 GHz	125.9 ± 0.2 GHz
1 ↔ 3	141.8 GHz	148.6 ± 0.3 GHz

This small discrepancy is attributed to interface effects such as the finiteness of the potential barrier and the true behavior of the polarization interaction at small distances. In order to take into account these effects several model calculations have been performed to fit the experimental results, In particular, Hipólito et *al.*[16] have obtained an exact solution, in terms of confluent hypergeometric functions, for the following model potential

$$V(z) = \begin{cases} -\dfrac{Qe^2}{(z+\beta)} & z > 0 \\ V_0 & z \leq 0 \end{cases} \qquad (2.6)$$

where β is an adjustable parameter. This model potential corresponds to treating the potential outside the surface as an image potential with the origin at a small distance β inside the dielectric. In fact, β is interpreted as being the position of the center of mass of the induced charge, That is the effective position of the interface. Thus, this phenomenological potential eliminates the non-physical divergence of the classical image potential at the real interface. When the eigenvalue equation is solved as a function of β for the levels n = 1, 2 and 3 and the energy separations between these levels are set equal to the experimental values, the parameter β takes the value 1.01 Å.

In the experimental situation there is an additional potential coming from an external electric field F pressinç the electronsagainst the surface and distorting the fosm of the potential to

$$V(z) = -\frac{Qe^2}{(z+\beta)} + eFz \qquad (2.7)$$

Since there is no exact analytical solution for this problem, we have performed numerical calculations of the bound-state energies for the levels 1, 2 and 3, in the presence of the applied electricfield and with the value of β previously calculated. In fig. 1, we show the transitions, from the ground-state to excited levels as observed in the experiments of Grimes et *al.*[15]. The spectrum looks like the Lyman series of the hydrogen atom. We plot in fig. 2 the transition frequencies as a function of the external electric field applied between two planar

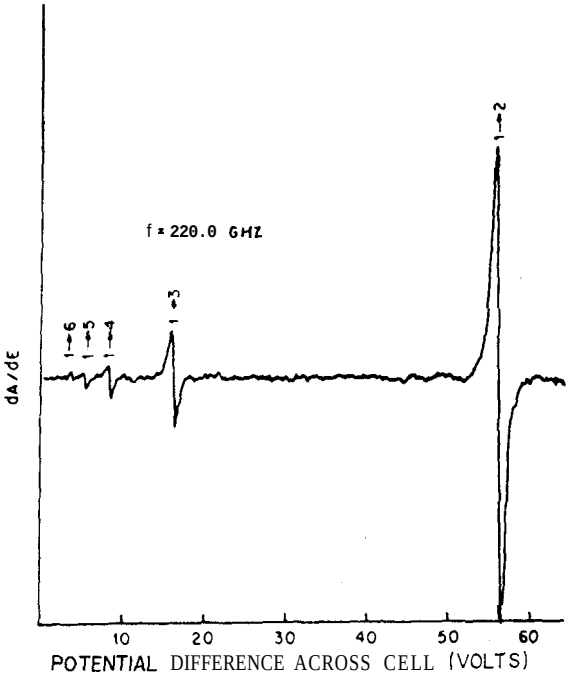

Fig.1 - Experimental recording of mm-wave absorption derivative vs the potential difference across the experimental cell taken at a frequency of 220 GHz and temperature of 1.2 K. The linear Stark effect is employed to tune the splittings between bound electronic surface states on liquid helium to resonance with the applied radiation. The $1 \rightarrow 2$, $1 \rightarrow 3$, ... transitions are analogous to the Lyman α, β, ... transitions of the hydrogen atom (After C.C. Grimes *et al*, ref.15).

electrodes one located above the surface and another inside the liquid, The energy separations between the lowest subband and the lowest few excited subbands are compared with those obtained numerically. As onesees, the experimental results are well fitted by the calculation.

The most striking feature of this system is the experimental accessible range of electron densities $n \sim 10^5 - 10^9$ cm^{-2}. As the 2D Fermi energy is given by

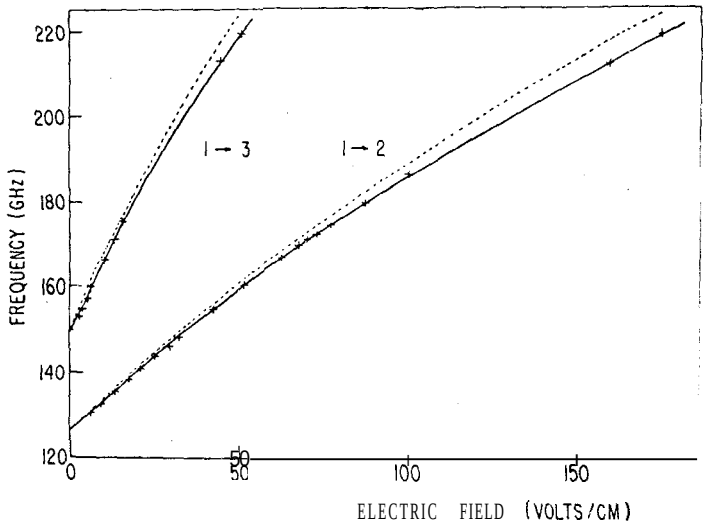

Fig.2 - Frequencies for the transitions $1 \rightarrow 2$ and $1 \rightarrow 3$ as a function of external field. The crosses are the experimental results of Grimes et al.[15] while the dashed curves are their model calculation. The solid curvesare the results of Hipólito et al.[16] based on the exactly soluble model potential given by eq. (2.6).

$$E_F = (\pi\hbar^2/m)n \tag{2.8}$$

then $E_F << k_B T$ for temperatures above a few millikelvins. Indeed, the electron system behaves like a non-degenerate plasma described by a two-dimensional Boltzmann distribution as a limit of the Fermi distribution at experimental densities and temperatures. In this way, the system can be characterized by a plasma parameter Γ defined as the ratio between the averages of potential and kinetic energies,

$$\Gamma = \frac{\langle\phi\rangle}{\langle K\rangle} = \frac{e^2(\pi n)^{1/2}}{T} \tag{2.9}$$

(T in energy units). For small values of Γ the Coulomb interaction is less important and we have a dilute system at high temperature. At intermediate densities, $1 < \Gamma < 100$, the system becomes highly correlated,

or liquid-like. At high densities and low temperature, a phase-transition to an ordered state, the classical Wigner crystal, is expected to occur. In fact, one of the most important development in this field has been the observation of the crystalization of electrons by Grimes and Adams[17] at $\Gamma_m = 137$. This result is consistent with calculations carried out using molecular dynamics[18] and Monte Carlo[19] computer simulations, We shall come back to this point in section 6 in the contextof the helium films.

The simplest approximation to treat a 2D classical plasma with particles interacting via a pair potential $\phi(r) = e^{*2}/r$, is the Random -Phase Approximation (RPA). The effects of the helium substrate are included into the renormalized electron charge $e^* = (2/1+\varepsilon)^{1/2} e$. In some sense, this approximation is equivalent to the Debye-Hückel method and it is known to be valid in the low density regime. In the dielectric formulation of the many-body problem, the dielectric function $\varepsilon(\vec{q},\omega)$ is related to the density-density response function $\chi(\vec{q},\omega)$ by

$$\left[1/\varepsilon(\vec{q},\omega)\right] - 1 = \phi(\vec{q})\ \chi(\vec{q},\omega) \tag{2.10}$$

where $\phi(q)$ is the Fouriei transform of the bare potential. The dielectric response function in RPA is usually calculated on the basis of the Vlasov equation and will be derived in a more general context in section 4. In RPA, the dielectric function turns out to be

$$\varepsilon(\vec{q},\omega) = 1 - \phi(\vec{q})\ \chi_0(\vec{q},\omega) \tag{2.11}$$

where $\chi_0(\vec{q},\omega)$ is the density-density response function of the ideal gas, given by

$$\chi_0(\vec{q},\omega) = -\ (n/T)W(z) \tag{2.12}$$

where $z = (\omega/q)(m/T)^{1/2}$. Here, $W(z)$ is the plasma dispersion furiction written as

$$W(z) = \frac{1}{(2\pi)^2} \int_{-\infty}^{+\infty} dx\ \frac{x\, e^{-x^2/2}}{x - z - i\eta}$$

The static structure factor $S(\vec{q})$ is related to the imaginary part of the density-density response function of the system through the well-known fluctuation-dissipation theorem

$$S(\vec{q}) = -\frac{\hbar}{2\pi n}\int_{-\infty}^{+\infty} d\omega \ \mathrm{Im}\ \chi(\vec{q},\omega)\ \coth\left(\frac{\hbar\omega}{2T}\right) \tag{2.13}$$

In the classical limit $\hbar\omega << T$, this function can be written by means of the Kramers-Kronig relation as

$$S_{RPA}(q) = q/(q+k_D) \tag{2.14}$$

where $k_D \approx 2\pi n e^2/T$ is the Debye wavevector.

The pair correlation function $g(r)$, which represents the propability of finding one particle at a distance r from another one, is obtained from the inverse Fourier transform as

$$g(r) = 1 + (1/2\pi n)\int_0^{\infty} k dk\ J_0(kr)\left[S(k)-1\right] \ . \tag{2.15}$$

In RPA, $g(r)$ is given by[20]

$$g_{RPA}(r) = 1 - U(r)/T \tag{2.16}$$

with

$$U(r) = (e^2/r)\ \{1-(\pi/2)k_D r\left[\bar{H}_0(k_D r)-Y_0(k_D r)\right]\}$$

where $\bar{H}_0(x)$ and $Y_0(x)$ are respectively the zero-order Struve and Bessel functions of second kind. So, the pair correlation function diverges as $-e^2/Tr$ near the origin, contrary to the exponential 3D behavior. This divergence is strongly manifested in the correlation energy E_c given by

$$E_c/nT = \pi\int_0^{\infty} r dr\ \ \phi(r)\left[g(r)-1\right] \tag{2.17}$$

which diverges logaritmically. This is a manifestation of the failure of the RPA in describing the features of the 2D electron plasma even

for small values of Γ. So, we cannot use this approximation intheshort -range domain $r \lesssim e^2/T$, where the electrons are strongly correlated, suggesting the importance of the short-range correlations in a 2D system. Furtherrnore, the pair correlation function which must be positive definite for all separations takes on negative values in this region. In 3D, a similar failure has less significant effects on the correlation energy, because the short-range domain does not contribute to its leading terms. Then, the inadequacy of RPA is much more significant in two than three-dimensional system,

From the zeros of the dielectric function one can determine the collective excitations of the system. In the long-wavelength limit and for small Landau damping, the plasma dispersion relation can be written as[21]

$$\omega = \omega_p + i\gamma_L$$

with

$$\omega_p^2 = \left(\frac{2\pi ne^2}{m}\, q\right)\left(1 + \frac{3q}{k_D}\right) \tag{2.18}$$

and

$$\gamma_L = \left(\frac{\pi}{8}\right)^{1/2} \left(\frac{k_D}{q}\right)^{1/2} \exp\left[-\frac{k_D}{2q} - \frac{3}{2}\right] \omega_p \tag{2.19}$$

This two-dimensional plasmon is very interesting because its dispersion and damping reflect the incomplete screening in 2D. Physically, plasmons are plane density waves propagating like lines of charge in 2D and sheets of charge in 3D. While the electric field required to restore charge uniformity is independent of the wavelength λ in 3D, it falls off as λ^{-1} in 2D. This gives a plasmon frequency which is independent of q in 3D and behaves like eq. (2.18) in 2D.

3. ELECTRONS ON THE SURFACE OF HELIUM FILMS

The spectrum of bound states changes significantly ifelectrons are put on a helium film covering a solid substrate with a dielectric constant ε_s, as shown in fig. 3. In this case, the substrate induces alterations in the image forces and one modifies the electronic states by varying only the thickness d of the film. The image potential can be

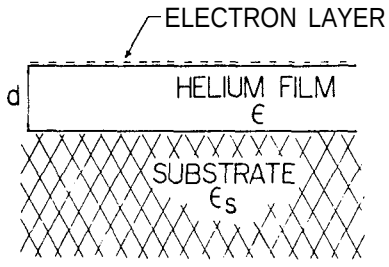

Fig.3 - Schernatic illustration of the geometric arrangement for the surface electrons on film of liquid helium adsorbeb on a substrate.

written as

$$V(z) = - \frac{Qe^2}{z} - Q_1 e^2 \sum_{\ell=0}^{\infty} \frac{(-a)^{\ell-1}}{z + \ell d} \qquad (3.1)$$

where $Q_1 = \varepsilon\delta/(\varepsilon+1)^2$ and $a = 4Q\delta$, with $\delta = (\varepsilon_s-\varepsilon)/(\varepsilon_s+\varepsilon)$. Since the series is rapidly convergent, one can retain only the first term.

A detailed analysis of the spectrum of the electronic stateson a helium film adsorved on a metal (δ=1) was given by Gabovich et al.[23]. For thick films, the condition $\langle z\rangle_n \ll d$ is satisfied and one can expand $V(z)$ as

$$V(z) = - Qe^2/z - Q_1 e^2/d + Q_1 e^2 z/d^2 \qquad (3.2)$$

So, in this limit, the substrate acts as an external pressing electric field $F_d = 1/d^2$. The presence of a large constant negative contribution $Q_1 e^2/d$ to the potential energy of the electron greatly increases the binding energy of electrons (11.6 meV for d = 300 Å) as compared with the bindingenergy of electronson bulk helium (0,7 meV). Due to the effective electric field $Q_1 e/d^2$ and the van der Waals forces coming from the substrate which stabilize the electron-film system (see sectíon 6) the maximum density to which the surface can be charged increases drastically[24].

The correction to the spectrum of electrons on bulk helium (eq. 2.4) is given by

$$\Delta\varepsilon_n(d) = - \frac{Q_1 e^2}{d} \left[1 - \frac{3}{2} \frac{\hbar^2}{mQe^2} \frac{n^2}{d} \right] \qquad (3.3)$$

which corresponds to a first-order Stark effect of the clamping field F_d.

For thin films, one can neglect the image forces in the helium film and the spectrum is determined by the image contribution of the substrate. In this situation the electron potential turns out to be the same as given by eq. (2.6) with Q and β replaced by Q_1 and d respectively. So, the energy levels differ markedly from the hydrogenüc spectrum and are given approximatedly by

$$\epsilon_n \approx \frac{me^4}{8Q_1\hbar^2}\left[n - \frac{3}{4} + \frac{1}{\pi}\left(\frac{2dme^2}{\hbar^2}\right)^{1/2}\right]^{-1/2} \tag{3.4}$$

for $d >> a$, and high quantum numbers.

It is obvious that the substrate will also affect appreciably the magnitude and nature of the interaction between the electrons in the plane. The bare potential between the electrons can now be found from the identity

$$\frac{1}{(r^2+z^2)^{1/2}} = \int_0^\infty J_0(qr)\, e^{-q|z|}\, dq$$

with appropriate boundary conditions for the potential and electric field[25]. The result, in q-space, is

$$\phi(q) = \frac{4\pi e^2}{q} F(qd) \tag{3.5}$$

where

$$F(qd) = \frac{1 - \delta e^{-2qd}}{(1+\varepsilon) - (1-\varepsilon)\delta\, e^{-2qd}} \tag{3.6}$$

with 6 defined through eq. (3.1). For electrons on the bulk helium ($d\to\infty$) we recover the usual poteritial for electrons confined in a plane

$$\phi(q) = \frac{2\pi e^{*2}}{q} \tag{3.7}$$

In the limit of thin helium films ($qd << 1$), $F(qd)$ assumes the form

$$F(dq) = \frac{1}{1+\varepsilon_s} + \frac{\varepsilon_s^2 - \varepsilon^2}{\varepsilon(1+\varepsilon_s)^2} qd \tag{3.8}$$

For a metal substrate, one obtains a potential wnich does not depend on q, that is

$$\phi(q) = \frac{4\pi e^2}{\varepsilon} d \tag{3.9}$$

Then, in this case the interaction between electrons is strictly dipolar, since in real space one can write

$$\phi(r) = \frac{e^2}{r} - \frac{e^2}{\left[r^2+4d^2\right]^{1/2}} \simeq \frac{1}{2} \frac{(ed)^2}{r^3} \tag{3.10}$$

We rnust note the drastic screening of the Coulcinb interaction coming from the substrate.

For a substrat'e with large dielectric constant $\varepsilon_s >> \varepsilon$, for example a semimetal, $F(qd)$ assumes the form

$$F(qd) = \frac{\varepsilon + \varepsilon_s qd}{\varepsilon \varepsilon_s} \tag{3.11}$$

As one can see, this system constitutes an excellentlaboratory to test many-body theories, since, by varying the film thickness and the particle density which are the experimentally accessible pararneters, one can change the nature of the bare interaction between the particles and the plasma parameter.

4. CORRELATIONS IN THE 2D CLASSICAL ELECTRON PLASMA

The static and dynamic properties of electrons on the surface of liquid helium were studied in references 26-28, As discussed in section 2, the short-range correlations are quite important in this system, so that an improvement of RPA is necessary. The calculations have been carried out on the basis of a kind of generalized random-phase approximation, the self-consistent-field method (SCFA) developed by Singwi and collaborators[10].

We start with the Liouville equation for the N-particle dis-

tribution function $f_N(\vec{r}_1, \vec{p}_1 \ldots \vec{r}_N, \vec{p}_N | t)$,

$$\frac{\partial f_N}{\partial t} + \left[\sum_{i=1}^{N} Q(\vec{r}_i, \vec{p}_i) \right] f_N = 0 \tag{4.1}$$

where the operator $Q(\vec{r}_i, \vec{p}_i)$ is defined as

$$Q(\vec{r}_i, \vec{p}_i) = \vec{v}_i \cdot \frac{\partial}{\partial \vec{r}_i} - \frac{\partial}{\partial \vec{r}_i} V_{ext}(\vec{r}_i, t) \cdot \frac{\partial}{\partial \vec{p}_i} + \frac{1}{2} \sum_{i \neq j} \frac{\partial}{\partial \vec{r}_i} \phi(\vec{r}_i - \vec{r}_j) \cdot \frac{\partial}{\partial \vec{p}_i} \tag{4.2}$$

and $V_{ext}(\vec{r}_i, t)$ is an external potential. Integrating the Liouville equation with respect to the coordinates and momenta of $N-1$ particles, one obtains the equation of motion for the one-particle distribution function $f_1(\vec{r}, \vec{p}, t)$

$$\frac{\partial f_1}{\partial t} + \vec{v} \cdot \frac{\partial f_1}{\partial \vec{r}} - \frac{\partial}{\partial \vec{r}} V_{ext}(\vec{r}, t) \cdot \frac{\partial f_1}{\partial \vec{p}} - \int d\vec{r}' d\vec{p}' \frac{\partial}{\partial \vec{r}} \phi(\vec{r} - \vec{r}') \cdot \frac{\partial f_2}{\partial \vec{p}} = 0 \tag{4.3}$$

where $f_2(\vec{r}, \vec{p}, \vec{r}', \vec{p}' | t)$ is the two-particle distribution function. The equation of motion for f_2 contains, in turn, the three-particle distribution function and so on. In the SCFA, this infinite hierarchy of equations is truncated by decoupling the two-particle distribution function through the ansatz

$$f_2(\vec{r}, \vec{p}, \vec{r}', \vec{p}' | t) = f_1(\vec{r}, \vec{p}, t) f_1(\vec{r}', \vec{p}', t) g(\vec{r} - \vec{r}') \tag{4.4}$$

where $g(\vec{r} - \vec{r}')$ is the static pair correlation function, With this ansatz, the short-range correlations are included, in an approximate way, through $g(\vec{r} - \vec{r}')$ which gives a measure of the probability of finding a second particle at a position $\vec{r}'$ when the first one is at $\vec{r}$. Assuming $g(\vec{r}) = 1$ for all $\vec{r}$ in eq. (4.4) is equivalentto the decoupling of f_2 in RPA and leads to the Vlasov equation.

We assume now that

$$f_1(\vec{r}, \vec{p}, t) = f_0(\vec{p}) + \delta f(\vec{r}, \vec{p}, t) \tag{4.5}$$

where $f_0(p)$ is the equilibrium distribution function and δf represents the deviation of f_0 induced by the weak external potential. Using eqs. (4.4) and (4.5) one linearizes the equation of motion. Proceeding in the standard way, one obtains the induced particle density in Fourier space as

$$\delta n(\vec{q},\omega) = \chi(\vec{q},\omega) V_{ext}(\vec{q},\omega) \tag{4.6}$$

where $\chi(\vec{q},\omega)$ is the density-density response function given by

$$\chi(\vec{q},\omega) = \frac{\chi_0(\vec{q},\omega)}{1 - \psi(\vec{q})\chi_0(\vec{q},\omega)} \tag{4.7}$$

The effective potential $\psi(q)$ is related to the structure factor $S(q)$, the Fourier transform of $g(r)$, through the expression

$$\psi(\vec{q}) = \phi(\vec{q}) + \frac{1}{n}\int \frac{\vec{q}.\vec{k}}{q^2}\,\phi(\vec{k})\,\left[S(\vec{q}-\vec{k}) - 1\right]\frac{d\vec{k}}{(2\pi)^2} \tag{4.8}$$

The second term of eq. (4.8) is responsible for the local field effects due to short-range correlations neglected in RPA, which is recovered by setting $\psi(\vec{q}) = \phi(\vec{q})$ in eq. (4.7). In this sense RPA is a trivial special case of the SCFA.

As before, the fluctuation-dissipation theorem (eq. (2.13)) and Kramers-Krönig relation put together allow us to write the density-density response function at zero frequency as

$$\chi(\vec{q},0) = -(n/T)S(\vec{q}) \quad , \tag{4.9}$$

so that the structure factor turns out to be

$$S(\vec{q}) = \frac{1}{1 + (\frac{n}{T})\psi(\vec{q})} \tag{4.10}$$

This completes the SCFA scheme. The equations (4.2) and (4.4) have to be solved numerically in a self-consistent way. From $S(\vec{q})$, the

pair correlation can be evaluated simply by a Fourier transformation operation.

For the electron gas on bulk helium, we can write the self-consistent equations in a similar way to the 3D classical electron .plasma, i.e.

$$S(q) = \frac{q}{k_D + q - G(q)} \tag{4.11}$$

where $G(q)$ is the local field function defined by the relation

$$\psi(q) = \phi(q)\ [1 - G(q)] \tag{4.12}$$

such that

$$G(q) = -\frac{1}{\pi^2 n}\left\{\int_0^q kdk\ E(\frac{k}{q})\ [S(k)-1] + q\int_q^\infty dk\left[\left(1 - \frac{k^2}{q^2}\right) K(\frac{q}{k}) + \left(\frac{k^2}{q^2}\right) E(\frac{q}{k})\right]\ [S(k) - 1]\right\} \tag{4.13}$$

where $K(x)$ and $E(x)$ are the complete elliptic integrals of the First and second kind respectively.

The self-consistent solution is obtained by the standard method of iteration. With a reasonable input $S(q)$, the effective potential $\psi(q)$ is calculateci and from it a new $S(q)$ is obtained. The procedure is repeated until self-consistency in $S(q)$ is achieved.

For the bulk helium case the pair correlation function is plotted in fig. 4 for severa1 values of the plasma parameter Γ. The results agree satisfactorily with those obtained from Monte Carlo simulations[29]. Note that, contrary to RPA results, our $g(r)$ is positive for all separations.

The influence of the film thickness on the self-consistent structure factor for two different substrates (metal and glass) is shown in fig. 5 and 6. In these figures, the film thickness is in unitsof the core radius $a = (\pi n)^{-1/2}$. For $d > 100$, $S(q)$ is independent of the nature of the substrate and similar to that of the strictly 2D electron gas.

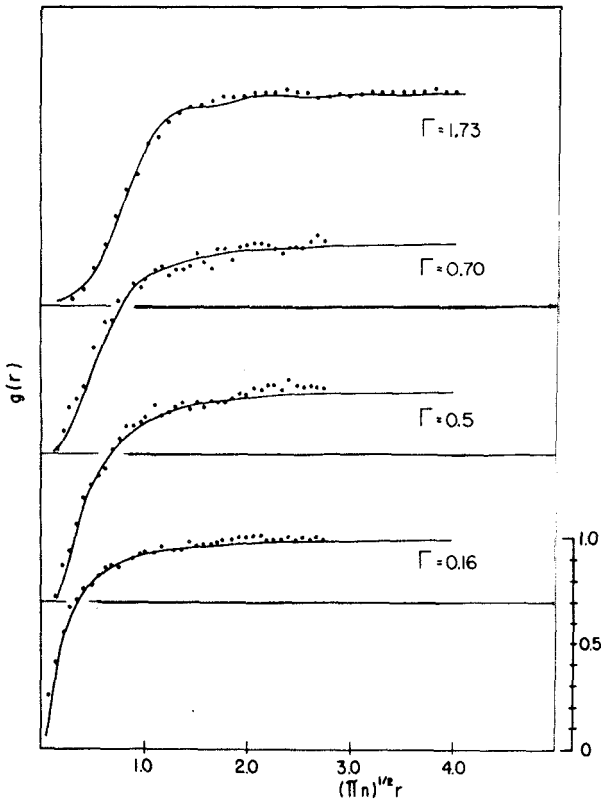

Fig. 4 - Pair correlation function $g(r)$ as a function of r in units of $(\pi n)^{-1/2}$ forseveral values of theplasma parameter, Thepoints are the Monte Carlo results.

For $1 < d < 100$, the differences in $S(q)$ for the two substrates are found only for small 4.

From $S(q)$ obtained self-consistently, the correlation energy can be evaluated as

$$E_c = (n/4\pi) \int_0^\infty k dk \; \phi(k) \; [S(k) - 1] \qquad (4.14)$$

In fig. 7, we present the results for the correlation energy density E_c/nT as a function of the film thickness for a metal substrate.

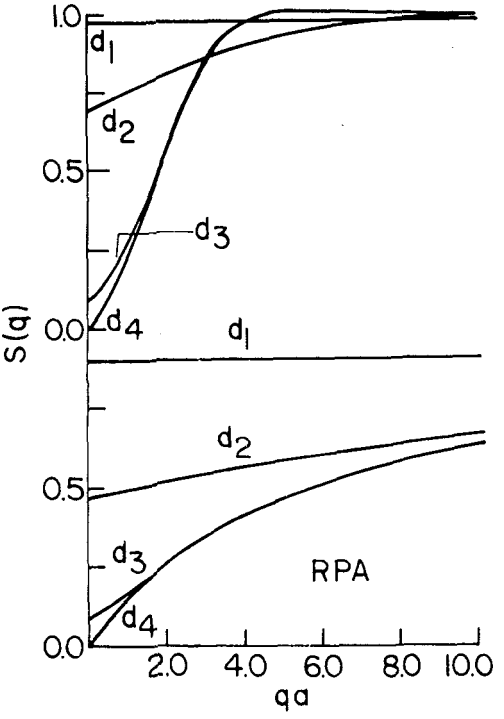

Fig. 5 - Structure factor $S(q)$ in both Self-Consistent-Field- Approximation (SCFA) and Random-Phase- Approximation (RPA) for several values of the film thickness (d_1 = 0.01, d_2 = 0.1, d_3=1.0, and d_4 = 100) and plasma parameteri' =3, for a metal substrate.

The value $d_c \approx 100$ is our estimate of the critical thickness, above which the results turn out to be the same as in the bulk helium case.

From the poles of the density-density response function, one can get the dispersion relation for the plasmons. In the long wavelength limit and for weak damping,

$$\omega_p^2 = (n/m)\ q^2\ \psi(q)\ \left[1 + 3\Gamma/n\ \psi(q)\right] \qquad (4.15)$$

In fig. 8, we show the results of the plasma dispersion relation for $\Gamma = 3$ and a metal substrate. In the limit of thin films, we

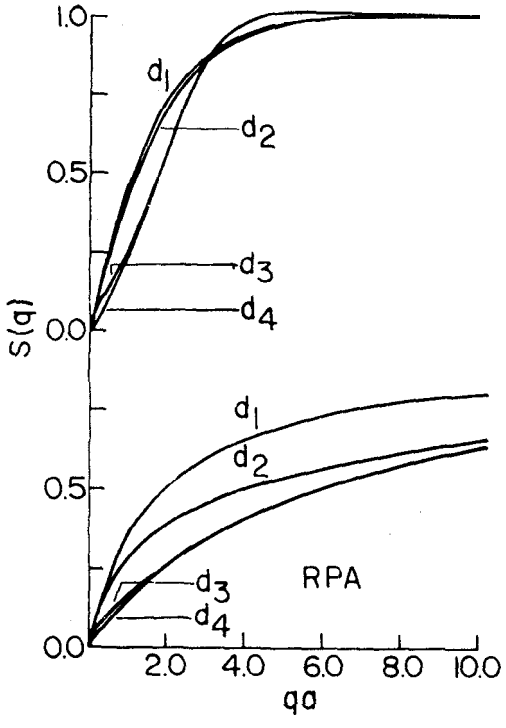

Fig.6 - Structure factor $S(\vec{q})$ for a glass substrate. The parameters are the same as those in fig. 5.

observe an unusual acoustical mode $\omega_p = cq$ with

$$c = c_0(1 + 3T/2mc_0^2) \tag{4.16}$$

where $c_0 = (\alpha/2)^{1/2} \cdot v_T$. Here $a = [1-S(0)]/S(0)$ is the fractional deviation of the constant $S(q)$ and $v_T = (2T/m)^{1/2}$ is the thermal electron velocity. In RPA[30], $\alpha_{RPA} = 2K_D d/\varepsilon$.

Increasing the film thickness, the long range interactioncomes to be quite important until the bulk limit is reached, with

$$\omega_p = (2\pi ne^2 q/m)^{1/2} [1 + (3/2 - \gamma)q] \tag{4.17}$$

where $\gamma = (1/4\pi n)\int_0^\infty dk\,[S(k)-1]$ is the correction to RPA due to short-range effects.

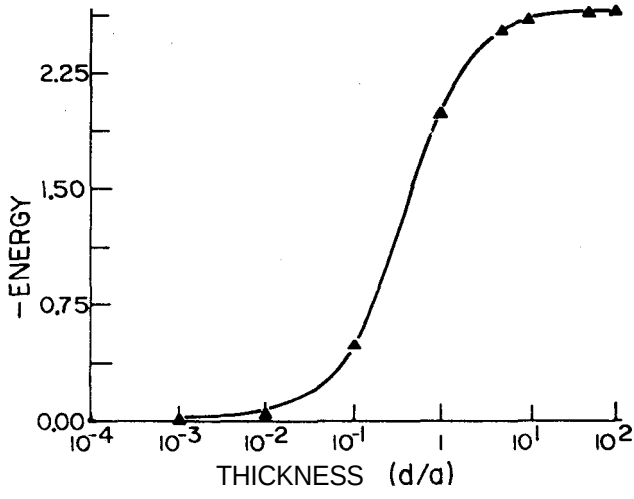

Fig. 7 - Correlation energy density E_c/nT as a function of thickness for a metal substrate and $\Gamma = 3$. The line is a guide to the eye. Note that the assymptotic limit corresponds to the bulk limit.

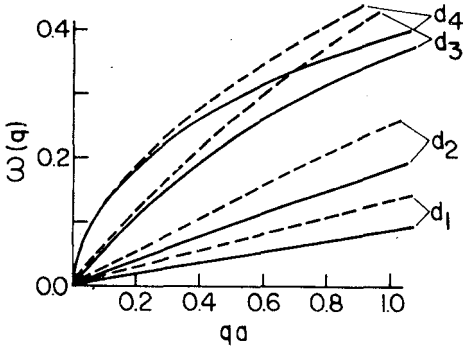

Fig.8 - Long-wavelength dispersion relation curves in units of $\omega_0 = (2\pi ne^2 k_D/m)^{1/2}$ for a metal substrate. The dashed lines are the results from RPA. The parameters are the same as those of fig. 5. Observe the transition from an acoustical mode to an usual 2D plasmon.

5. POLARONIC EFFECTS

The quantum electronic states described in previous sections are formed by assuming a planar liquid boundary. However, a perturbation of the surface profile, due to the presence of the normal modes of oscillation of the liquid surface, modifies the form of the wave equation [eq. (2.2)] governing the motion of electrons. We will describe now the electron interaction with these excitations, called ripplons, which are the quantized capillary-gravity waves of the helium surface. First, we consider a single electron picture for the electron-ripplon coupling, disregarding the electron-electron interaction, Later, the Coulornb interaction between localized electrons over the deformed surface will be introduced.

The ripplons are bosons with a dispersion given by

$$\omega^2 = [g'q + (\sigma/\rho)q^3] \tanh qd \qquad (5.1)$$

where q is the ripplon wave vector, a the surface tension, ρ the density of liquid helium. The van der Waals acceleration $g' = g+f$, where g is the acceleration of gravity and $f = 3\alpha/\rho d^4$, with a the van der Waals constant responsible for the attractive forces exerted on the helium atom from the side of the substrate.

In terms of the ripplon creation and annihilation operator a^+ and a_q, the displacement of the helium surface $u(\vec{r})$ can be written as [4]

$$u(\vec{r}) = A^{-1/2} \sum_q \Lambda_q (a_q^+ + a_q) e^{i\vec{q}.\vec{r}} \qquad (5.2)$$

where

$$\Lambda_q^2 = (\hbar q \tanh qd)/2\rho\omega_r$$

The treatment of electron-ripplon scattering based on the Born-Oppenheimer adiabatic principle, which takes into account the adjustment of the electronic states to the long wavelength oscillation of the liquid, has been discussed in detail by Shikin and Monarkha[22].

The electron-ripplon iriteraction potential can be written in

the following form

$$V = A^{-1/2} \sum_{\vec{q}} (a_q^+ + a_{-q}) V_q(z) e^{i\vec{q}.\vec{r}} \tag{5.3}$$

where

$$V_q(z) = A_4 [-Qe^2/z^2 + Qe^2 qK_1(qz)/z + Q_1 e^2/(z+d)^2 + eF] \tag{5.4}$$

and $K_1(z)$ is the modified Bessel function of second kind. At low temperature and high external electric fields, the electron-ripplon interaction can induce a self-localized electronic surface state. The electron deforms the helium surface forming a small dimple in which it localizes itself[31,32]. This electron-ripplon bound complex is called a polaron.

In the long wavelength limit where experiments have been performed, the motions parallel and perpendicular to the surface can be separated, and the polaron is described by a Frohlich type Hamiltonian as

$$H = (p^2/2m) + \sum_{\vec{q}} \hbar \omega_r a_q^+ a_q + A^{-1/2} \sum_{\vec{q}} V_q (a_q^+ + a_{-q}) e^{i\vec{q}.\vec{r}} \tag{5.5}$$

with

$$V_q = \Lambda_q (eF + Q_1 e^2/d^2) \tag{5.6}$$

The path-integral formalism, as introduced by Feynman for the polaron problem, was first worked out by Farias[33] and later by Hipólito et al.[34] in order to evaluate the ground-state energy and effective mass of the polaron,

The application of the Feynman theory to this specific problem was motivated by the fact that Feynman's treatment isthemost successful overall theory of the optical polaron, giving the lowest upper bound to the ground state energy, In this method, the ripplon coordinates are exactly eliminated in favor of a non-linear retarded interaction of the electron with itself, The physical meaning of this interaction with the past is that the perturbation caused by the moving electron spend time to propagate in the medium.

The path integral arises in the calculation of the propagator (or the partition function for finite temperature)

$$IK = \int \mathcal{D}\vec{r}(\tau) e^{S} \tag{5.7}$$

which is the probability amplitude for the dynamical evolution of the system, If we know IK, the eigenvalues and eigenfunctions of the Hamiltonian would be, in principle, determined. If we let the "time" $\beta \to \infty$

$$IK \sim e^{-\beta E_g} \tag{5.8}$$

where E_g is the ground state energy.

The action S, corresponding to the polaron Hamiltonian, is given by

$$S = -\frac{1}{2}\int_0^\beta d\tau \left(\frac{d\vec{r}}{d\tau}\right)^2 + \frac{1}{2}\int \frac{d^2q}{(2\pi)^2} |V_q|^2 \int_0^\beta d\tau$$

$$\cdot \int_0^\tau ds \exp\left[-\omega_r(\tau - s)\right] \exp\left[i\vec{q}.(\vec{r}(\tau) - \vec{r}(s))\right] \tag{5.9}$$

Obviously the functional integral, being intractable, must be replaced by a simple exactly soluble functional S_0. The use of Jensen's inequality

$$\langle e^{F} \rangle \geq e^{\langle F \rangle} \tag{5.10}$$

allows us to obtain a variational upper bound on the ground state energy

$$E_g \leq E_0 - \lim_{\beta \to \infty} \langle S - S_0 \rangle \tag{5.11}$$

where $E_0 = \log \int \mathcal{D}\vec{r}(\tau) e^{S_0}$ and $\langle \ldots \rangle$ means average with weigth e^{+S_0}. Feynman was able to choose a model to calculate S_0 which contains the physical significance of the true action S. In this model, the so-called two-parameter model, instead of the electron being coupled to the normal modes of the medium, it interacts with a single fictitious particle via a spring, and the pair of particles are free to wander, The mass of the

extra particle and the spring constant are the variational parameters. After eliminating the coordinates of the fictitious particles, the trial action assumes the form

$$S_0 = -\frac{1}{2}\int_0^\beta d\tau \left(\frac{d\vec{r}}{d\tau}\right)^2 - \frac{C}{2}\int_0^\beta d\tau \int_0^\tau ds \cdot \exp\left[-\Omega(\tau-s)\right]\left[\vec{r}(\tau)-\vec{r}(s)\right]^2 \qquad (5.12)$$

For our specific electron-ripplon complex,

$$E_g \leq \frac{1}{v}(v-\Omega)^2 - \int \frac{d^2q}{(2\pi)^2}|V_q|^2 \int du\, e^{-\omega_r u} e^{-q^2 F(u)/2v^2} \qquad (5.13)$$

where

$$F(u) = \frac{v^2-\Omega^2}{v}(1 - e^{-vu}) + \Omega^2 u \qquad (5.14)$$

and v is defined in terms of the variational paraméter C and Ω as

$$v^2 = \Omega^2 + \frac{4C}{\Omega} \qquad (5.15)$$

The variational parameters Ω and C are determinedby minimizing the expression for the energy. The numerical calculations for the ground state energy of the polaron for films on a metal are shown in fig.9, as a function of the film thickness and for two values of the external electric field, The energies for films deposited on othersubstrates were also calculated and the result is that the influence of the substrate is significant only for $d \lesssim 500$ Å. When the film thickness is of the order of 50 Å the contribution of the substrate to the electric field totally dominates the external electric field, The main result is that in the limit of zero external electric field ($F=0$), the polaron energy in a metal substrate is greater than in any other substrate.

Similar calculations have been made by Jackson and Platzman[35] for one particular thickness of the film ($d \simeq 100$ 8). In order to get analitycal results in the strong coupling and weak coupling limits they introduced a cutoff $k_c = (\rho g'/\sigma)^{1/2}$ (a being the capillary constant), in the electron-ripplon interaction and approximated the ripplon dispersion [eq.(5.1)] by a sound like dispersion for $q < k_c$, They found a phase--transition like behavior from an electronic delocalized state to a

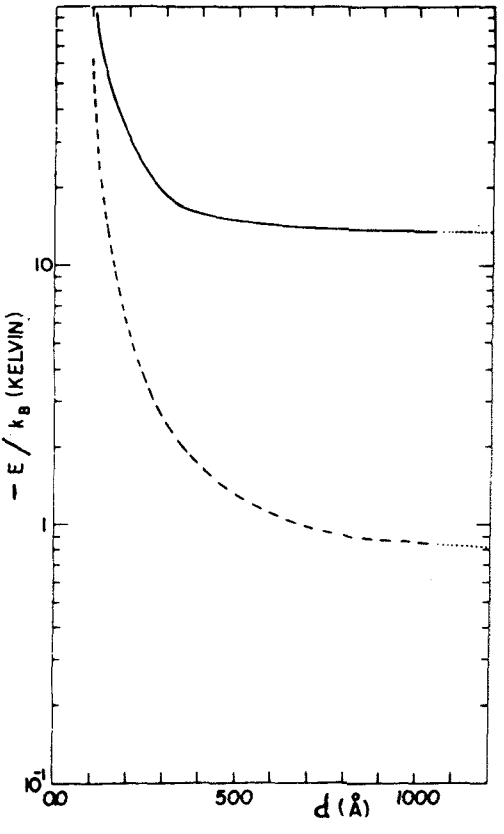

Fig.9 - Localization energy of an electron as functionof the thickness of the helium film on metallic substrate. Solid and dashed curves correspond to $F \simeq 20.0 \times 10^3$ V/cm and 5.0×10^3 V/cm.

self-trapped one at a critical value of the electron-ripplon coupling constant. This "localization" transition refered here is not to be taken literally, but rather in terms of the rapidity and magnitude of the change of the effective mass of the polaron over a narrow range of the coupling constant. Our numerical calculations using the path-integral formal ism were performed in terms of the experimental accessible variables, the externa1 electric field and film thickness, and do not include any kind of approximation in the electron-ripplon interaction or ripplon dispersion.

The properties of this polaron in high magnetic field havebeen

investigated by Saitoh with the use of path-integral methods[36].

Very recently Degani and Hipólito[37] have studied in detail the ground state properties with emphasis on this novel and interesting polaronic phase transition. They used a simple unitary-transformation formalism, based on a generalization of the variational approximation of Lee, Low and Pines, which was previously applied to the study of the surface polaron by de Bodas and Hipólito[38]. The advantage of this method is the great flexibility for applications to Hamiltonians similar to (5.5) with several kinds of interacticn potential and appropriate dispersion relation. It was demonstrated that this approximation gives the same results as Feynman's formalism in strong-coupling and weak-coupling limits for other types of polarons. Furthermore, this unitary-transformation method has been used in the study of the polaron phase transition

For the electron-ripplon ground state, the variational wavefunction $|\psi>$ is postulated as a product of an electron wavefunction and a coherent ripplon state, This surface state is not an eigenstate of the total parallel momentum operator $\vec{p}_t$,

$$\vec{p}_t = \vec{p} + \sum_{\vec{q}} \hbar \vec{q}\, a_q^+ a_q \tag{5.16}$$

where $\vec{p}$ is the electron momentum.

The minimization of the energy should be performed by constraining the operator $\vec{p}_t$ so that

$$\delta(<\psi|(H-\vec{\mu}.\vec{p}_t)|\psi>) = 0 \tag{5.17}$$

where $\vec{\mu}$ is the Lagrange multiplier (which ends up as the polaron velocity) introduced to keep the expectation value of the total momentum equal to a given constant,

The method consists first in subjecting the Hamiltonian $H = H - \vec{\mu}.\vec{p}_t$ to a canonical transformation S_1,

$$S_1 = \exp(-i\eta \sum_{\vec{q}} \vec{q}.\vec{r}\, a_q^+ a_q) \ , \tag{5.18}$$

where η is a variational parameter which recovers the weak-coupling ap-

proximation as $\eta=1$ and gives the strong-coupling theory in the limit $\eta \to 0$.

Next the expectation value of the resulting Hamiltonian iscalculated by choosing a variational wave function with the following form

$$|\psi\rangle = (m\lambda/\pi\hbar)^{1/2} \exp(-m\lambda r^2/2\hbar) \exp\left[-i(m\lambda/2\hbar)^{1/2}\vec{p}_0 \cdot \vec{r}\right] S_2 |0\rangle \qquad (5.19)$$

where $|0\rangle$ is the rippion ground-state wave function, obtained from $a_4|0\rangle = 0$ and $\langle 0 \mid 0\rangle = 1$, h and $\vec{p}_0$ are variational parameters and S_2 is the well-known second Lee-Low-Pines canonical transformation given by

$$S = \exp\left[\sum_{\vec{q}} (\xi_{\vec{q}} a_q^+ - \xi_{\vec{q}}^* a_q)\right] \qquad (5.20)$$

and $\xi_{\vec{q}}$ is a variational function to be determined,

Minimizing the energy with respect to the variational parameters λ and $\vec{p}_0$, up to second order in the velocity $\vec{\mu}$, we finally obtain the expressions for the ground-stete energy and effective mass given by

$$E_g = \frac{\hbar\lambda}{2} - \sum_{\vec{q}} \frac{|V_q|^2 \exp\left[-(1-\eta)^2\hbar q^2/2m\lambda\right]}{\hbar\omega_p + \eta^2\hbar^2 q^2/2m} \qquad (5.21)$$

and

$$m^* = m\left[1 + \hbar^2 \sum_{\vec{q}} \frac{q^2 |V_q|^2 \exp\left[-(1-\eta)^2\hbar^2 q^2/2m\lambda\right]}{(\hbar\omega_p + \eta^2\hbar^2 q^2/2m)^3}\right] \qquad (5.22)$$

This calculation formally reproduces the path-integral results provided one introduces the upper cut-off $k_c = \sqrt{\rho g^{-1}/\sigma}$ into the integration over q in eq. (5.13).

By analogy with the polaron problem we define a coupling constant a as

$$\alpha = me^2 F_T^2/4\pi\hbar^2 k_c^2$$

where $F_T = F + Q_1 e/d^2$. In the weak-coupling approximation α is small and $\eta = 1$. In this limit it is clear from eq. (5.17) that a minimum of E_g occurs at $\lambda = 0$. Then, for the energy and effective mass we obtain

$$E_g^{WC} \cong -2\gamma\alpha \quad , \quad \gamma = 2m\sqrt{g'd}/\hbar k_c \tag{5.23a}$$

$$m^*/m \quad 1 \tag{5.23b}$$

In the strong-coupling limit, corresponding to large values of α, $\eta \to 0$, the energy behaves like

$$E_g^{SC} \cong -\alpha + \sqrt{\alpha} + \ldots \tag{5.24a}$$

and the effective mass goes like

$$m^*/m \cong 1 + 2\alpha/\gamma^2 - \sqrt{\alpha}/\gamma^2 + \ldots \tag{5.24b}$$

In general, the energy, defined in eq. (5.17), is miriimized with respect to the variational parameters λ and η. Hence, with the best-fit values of those parameters the ground-state energy and the effective mass are obtained. In figs. 10 and 11 the results are plotted against the externa1 electric field for various values of the thickness of the helium film adsorbed in solid neon (and $k_c = 1.45\ 10^9/d^2\ \ cm^{-1}$). As we see from fig. 10, for each thickness of the helium layer the energy has two distinct branches corresponding to the stable solutions of eq. (5.21). The first branch, representing the weak-coupling ($\eta = 1$) regime, crosses the second one which corresponds to the strong-coupling, at a certain critica1 value of the clamping electric field F_c. At this crossing point there is a discontinuous change in the slope of the energy, characterizing a first-order phase-transitions behavior in which the polaron state transforms from a nearly-free to a localized state type. The extremely rapid variation at the critica1 point is more dramatically seen in fig. 11, where the effective mass, in units of the electron mass, changes by severa1 orders of magnitude.

Recent experimental measurements by Andrei[14] appear to corroborate this theoretical prediction by observing the localization of the

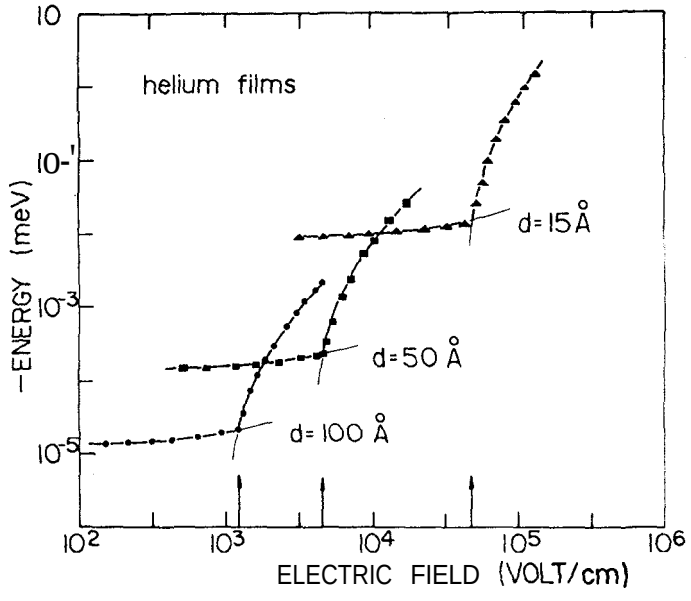

Fig, 10 - Ground-state energy as function of the clamping externa1 field for three values of the film thickness in the case where the substrate is solid neon ($E_s = 1.24$). Points are numerical results and lines are only guides to the eye.

electron as a polaronic state for $d < 1000$ Å and $0.4 < T < 1$ K. In her experiments Andrei makes measurements of the mobility and effectivemass of electrons on a helium film, She found that at certain critical point a sharp $4\frac{1}{2}$ order of magnitude drop in the mobility occurs, The electronic effective mass on the other hand increases by 8 orders of magnitude, characterizing the observation for the first time, of the transition to a surface polaron state as predicted by a single electron theory, Although the experimental measurements support the basic polaron model ideas, many electrons are present in the experimental situation, suggesting that Coulomb interaction between electrons playsan important role, introducing then a new scale of energy into the problem (the polaron state, with binding energy of the order of milikelvins, as we

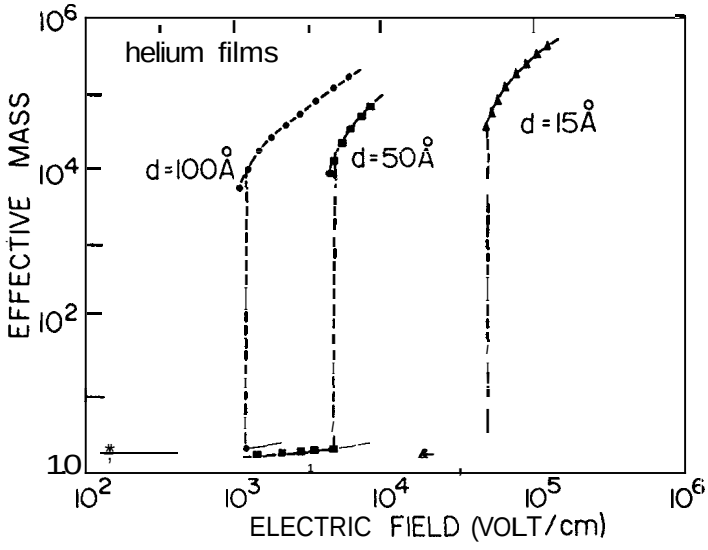

Fig.11 - Effective mass in units of the free electron mass as function of the external electric field for three values of the film thickness in the case where the substrate is solid neon. Points are numerical results and lines are guides to the eye.

have calculated before, is far too low to be observable at the experimental temperatures $0.4\ K \lesssim T \lesssim 1\ K$).

With many electrons present, an instability of the chasged helium surface can be generated by forming separate many-electron dimples within an energy scale which might allow experimental observation. Within the context of Andrei's experiment, we now describe the properties of an individual dimple filled with several electrons ($N \cong 40 - 90$) trapped at the surface of a helium film adsorbed on solid sapphire[39].

Since the effective charge of the dimple (Ne) and the mass (Nm) are large, the polaron coupling constant a becames proportional to the fifth power of the number of electrons N. In this case, the polaron is strongly bound to the surface even at zero external pressing electric field. Thus, from the strong-coupling regime of our model, we can obtain the total energy E_g associated with a many-electron dimple, justby adding to the one-particle energy given by eq. (5.21) with $\eta = 0$ the

energy of the Coulomb interaction U_c between electrons inside the dimple. The total energy is then straightforward evaluated and, in units of $\hbar^2 k_c^2/2M$, has the following form

$$E_g = \alpha \exp(1/\lambda) Ei(-1/\lambda) + U_c(\lambda) \tag{5.25}$$

where $Ei(x)$ is the Exponential Integral function and

$$U_c(\lambda) = \frac{N^2 e^2}{2} \int \frac{|\psi(r)|^2}{r} d^2r \Big/ (\hbar^2 k_c/2M) = MN^2 e^2 (\pi\lambda/2)^{1/2} \Big/ \hbar^2 k_c \tag{5.26}$$

Also, $M = Nm$ is the dimple mass, and $\psi(r)$ is given by eq. (5.19).

Minimizing the ground state energy, given by eq. (5.25), with respect to λ we finally find the total energy of the system

$$E_g = -3.18 \times 10^{-8} N^2 F_T^2 [\log(F_T/\pi^{3/2}\sigma k_c) - 1] \quad \text{eV} \tag{5.27}$$

and the Coulomb interaction energy

$$U_c = (NeF_T)^2/4\pi\sigma \tag{5.28}$$

which is of the order of magnitude of Kelvins.

From eq. (5.27) we conclude that for a simple dimple it is energetically advantageous (with $E_g < 0$) to be localized at the surface of the helium film if $F_T^2 > 15.14\ \sigma k_c$. For bulk helium ($d \to \infty$) the minimum external field necessary to localize a dimple is $F_c = 3120$ V/cm, which is consistent with the experimental observation of Leiderer et al.[40].

In fig. 12 we show the results for the total energy, given by eq. (5.27), as function of the helium film thickness, for $F = 80$ V/cm and for several values of the number of electrons inside the dimple. Notice that, for each number of electrons in the dimple, there is a critical thickness of the helium film above which the energy becomes positive, and therefore, the dimple can not exist in a stable form. The criterion for the stability of the charged surface is, on the otherhand, related to the average density of charges above the surface, There is a critica1 concentration n_c of charges,

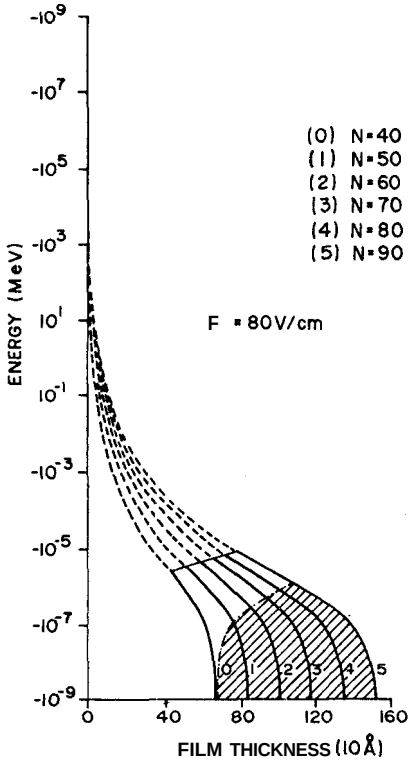

Fig. 12 - Binding energy of a single dimple filled with N electrons as function of the helium film thickness for an electric field F = 80 V/cm. The dashed part of each curve corresponds to an unstable solution where the average electron density is larger than the critica1 density n_c. The solid curves rspresent the film thickness regions where the dimple is stable. Tht: shaded region corresponds to Andrei's experimental region ($n = 10^8\,cm^{-2}$) where a dimple with more than 40 electrons can be formed.

$$n_c = (k_c \sigma^2 / 2\pi^2 e^2 \varepsilon_s)^{1/2} \qquad (5.29)$$

above which the dimple is not stable. For $n = n_c$ the surface becomes unstable at a wave vector $k_c = (3g'/\sigma)^{1/2}/d^2$. In fig. 13, the density n is plotted as a function of film thickness, critica1 density n_c and the experimental concentration $n = 10^8$ cm^{-2} recently used by Andrei[14]. It is clear from our results that the appearance of a stable many-electron dimple is limited by film thickness as well as by the electron density above the surface. From fig. 13, we note that, at experimental densities, only dimples with more than $N = 40$ electrons can be formed on the surface of the helium film. We can also see the rapid increase of the density with decreasing critical thickness. Consequently, at smaller thickness the electrons become more concentrated at the center of the

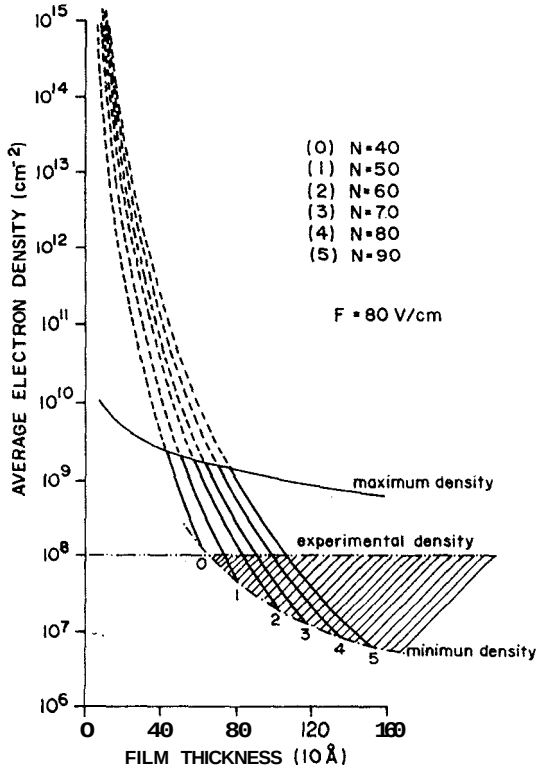

Fig.13 - Average electron density of a single dimple as function of the film thickness for an external electric field F = 80 V/m. The curves are described in the same way as in fig. 12.

dimple and the whole structure of the dimple becomes sharper, as can be seen directly from the average radius R of the multi-electron dimple

$$R = \int |\psi(r)|^2 \, r d^2 r = (2\pi^3)^{1/2} \, \sigma / F_T^2 \qquad (5.30)$$

Finally, we can verify from eqs. (5.27) and (5.30) that the existence of a stable multi-electron dimple is possible under the condition $k_c R \lesssim 1/2$. This means that the size of the region containing the

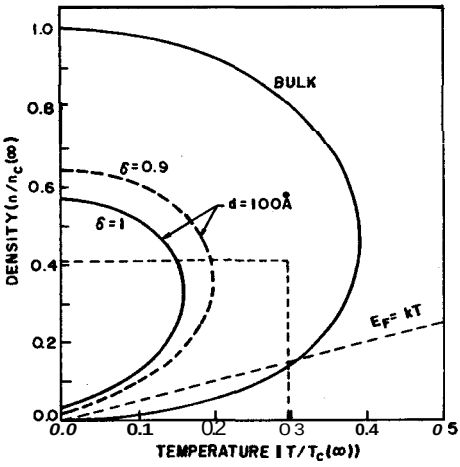

Fig. 14 - The phase diagram for bulk helium and for a c? = 100 Å film lying on two substrates (sapphire δ=0,9 and metal δ=1). n_c = 2.4 × 10^{12} cm^{-2} and T_c=33 K. (After Peeters and Platzman ref. 41).

electrons is smaller than a typical ripplon wavelength, justifying the validity of our model calculation.

6. THE PHASE-DIAGRAM

Very recently, the phase diagram of electrons on helium films has been investigated[39]. As we have discussed in section 2, a striking feature of the behavior of these surface electrons is the possibility that they can undergo a phase transition from a liquid phase to an ordered state as one increases the density or lowers the temperature for a fixed density, i.e., for large values of the plasma parameter Γ. This classical freezing transition has been observed for electrons on bulk helium[17]. The mechanism of this transition has been proposed in a seminal paper of Kosterlitz and Thouless (KT)[42] and later elaborated on by Halperin and Nelson (HN)[43]. This classical transition occurs by unbinding of dislocation pairs at Γ_m to a new phase, a liquid-crystal phase, with no long-range translational order but with bond orientational order. At $\Gamma = \Gamma_i$, the system undergoes another transition by unbinding of

disclination pairs to the usual liquid with no long order. The value of Γ_m is given, in the contex of KTHN theory as

$$\Gamma_m \sim \frac{1}{c_t^2}\left[1 - \frac{c_t^2}{c_\ell^2}\right]^{-1} \tag{6.1}$$

where c_t and c_ℓ are the transversal and longitudinal sound velocity of the solid, These constants must be renormalized by taking into account the effects of creation of defects in the solid. Using zero temperature values of c_t and c_ℓ, Thouless[44] found out a transition at Γ_m - 79. More refined numerical calculations by Morf[18], who solved the renormalization group equations of HN, raise the melting transition to $\Gamma \sim 125$ which is consistent with the experimental result.

On the other hand, there is a region of the phase diagram where the Fermi energy is larger than the thermal energy, $E_F >> T$, i.e., a low temperature phase where the Fermi energy dominates the kinetics of the electron system.

This region cannot be reached experimentally for electrons on bulk helium, because an dectrohydrodynamic instability of the charged surface occurs. This instability arises when one considerstheinfluence of the electrons on the dispersion relation of ripplons. It is expected that the frequency of ripplons with a wave vector around k_c (theinverse of the cappilary length) is considerably lowered as the electron density is increased. Indeed, for $n > n_c$, the frequency becomes imaginary, suggesting that the surface becomes unstable against deformations. For bulk helium $n_c = (\sigma g \rho)^{1/4}/(2\pi e^2)^{1/4} \approx 10^9$ cm^{-2} [45]. However, for electrons on helium films, the van der Waals helium-substrate interaction is incorporated in the dispersion relation of ripplons and drastically increases the critical density n_c. Remember that, in this case g, the gravitational constant, is replaced by $g = 3\alpha/\rho d^4$. For thin films n_c is given by eq. (5.29). So, the quantum region of the phase diagram can be achieved for electrons on thin helium films. Indeed, a recent experiment[46] has demonstrated that electron densities up to 10^{11} cm^{-2} above saturated films on both insulating and conducting substrates are stable.

Peeters and Platzman[39] have proposed a phase diagram of electrons on helium films by using a simple dimensional argument and KTHN theory. According to them, the relation

$$\langle\phi\rangle_d / \langle K\rangle = \Gamma_m(d) \tag{6.2}$$

must hold in the gas phase, where $\langle\phi\rangle_d$ is the potential energy given by eq. (3.5). Now, the eq. (6.1) turns out to be

$$\Gamma_m(d) = \Gamma_m(\infty)\, \frac{c_t^2(\infty)}{c_t^2(d)} \left[1 - \frac{c_t^2(d)}{c_\ell^2(d)}\right]^{-1} \tag{6.3}$$

where $c_t(d)$ and $c_\ell(d)$ are the zero-temperature sound velocities in a solid formed by particles interacting via a potential ϕ_d, and $\Gamma_m(\infty)$ is taken as the experimental result for electrons on bulk helium. The phase diagram is displayed in fig. 14. These are qualitative results, because they must take into account the values of sound velocities at finite temperature, where the renormalization effects in these constants are quite important. One important conclusion is that for a metal substrate one finds a fluid-like region as $n \to 0$ and $T \to 0$ for small film thickness. At high densities the solid melts again at a density n_w where the quantum transition occurs. These densities depend upon d in such a way that for $d \sim 70$ Å, the solid region shrinks to a point. This is an effect of the dipolar interaction at small film thickness. It is very interesting to analyse the quantum properties of a dipole gas of electrons which, now, has a physical experimental realization. The study of this system is in progress[47].

Most of the work described here has been done in collaboration with G.A. Farias, J.P. Rino, J.R. Drugowich de Felício and M. Degani. We would like to acknowledge them for valuable discussions and friendly cooperation. We would like to thank S.A. Jackson and M. Saitoh for helpful discussions on the polaronic state and E.A. Andrei for conver-

sations about her beautiful experiment. We also thank to Professor R.C. T. da Costa for a critical reading of the manuscript.

This work was supported by FAPESP and CNPq (Brazilian Government Agencies).

REFERENCES

1. M.W.Cole and M.H.Cohen, Phys. Rev. Lett. 23, 1238 (1969).
2. V.B. Shikin, Zh.Eksp.Teor.Fiz. 58, 1748 (1970) [Sov.Phys. JETP 31, 936 (1970)].
3. C.C.Grimes and T.R.Brown, Phys.Rev.Lett. 32, 280 (1974).
4. M.W.Cole, Rev.Mod.Phys. 46, 451 (1976).
5. C.C.Grimes, Surf.Sci. 73, 379 (1978).
6. V.B.Shikin and Yu. P. Monarkha, Fiz.Nizk.Temp. *1*, 957 (1975) [Sov.J. Low Temp. Phys. 1, 459 (1975)]
7. Yu. P. Monarkha and V.B.Shikin, Fiz.Nizk.Temp. 8, 563 (1982) [Sov. J.Low Temp.Phys. 8, 279 (1982)].
8. F.I.B. Williams, J.Phys. (Paris) 41, Colloques C3-249 (1980).
9. T.Ando, A.B.Fowler and F.Stern, Rev.Mod.Phys. 54, 437 (1982).
10. K.S.Singwi, M.P.Tosi, R.H.Land and A.Sjölander, Phys. Rev. *176*, 586 (1968). See also K.S.Singwi and M.P.Tosi in Solid St. Phys., vol.36, p.177, edited by Ehrenreich and Turnbull, Academic Press (1981).
11. R.P.Feynman, Phys.Rev. 97, 660 (1955). See also R.P.Feynman, *Statistical Mechanics*, ch. 8, Benjamin (1972).
12. R. Manka and M.Suffczynski, J.Phys. C 13, 6369 (1980).
13. O. Hipólito, J.Phys. C 12, 4667 (1979).
14. E.Y.Andrei, Phys. Rev. Lett. 52, 1449 (1984). See also E.Y. Andrei, C.C.Grimes and G.Adams, Surf. Sci. 142, 104 (1984).
15. C.C.Grimes, T.R.Brown, M.L.Burns and C.L.Zipfel. Phys. Rev. B 13, 140 (1976).
16. O. Hipólito, J.R.D. de Felício and G.A. Farias, Solid St. Comm. 28, 365 (1978).
17. C.C.Grimes and G.Adams, Phys.Rev.Lett. 42, 795 (1979).
18. R.H. Morf, Phys.Rev.Lett. 43, 931 (1979).
19. R.C.Gaan, S.Chakravarty and G.V.Chester, Phys, Rev. B*20*, 326 (1979).

20. N. Studart, PhD. Thesis - IFQSC/USP (1979) unpublished.
21. A.L.Fetter, Phys.Rev. B 10, 3739 (1974).
22. V.B.Shikin and Yu.P.Monarkha, J.Low Temp.Phys. 16, 193 (1974).
23. A.M.Gabovich, L.G. Il'chenko and É.A.Pashitskii, Zh.Eksp.Teor. Fiz. 81, 2063 (1981) [Sov.Phys.JETP *54*, 1089 (1981)]
24. H.Ikezi and P.M.Platzman, Phys.Rev. B*23*, 1145 (1981).
25. W.R.Smythe, *Static and Dynamical Electricity* p.192 - Mc-Graw Hill, New York (1950).
26. N. Studart and O. Hipólito, Phys. Rev. A 19, 1790 (1979).
27. N. Studart and O. Hipõlito, Phys. Rev. A 22, 2860 (1980).
28. J.P. Rino, N. Studart and O. Hipõlito, Phys. Rev. B 29, 2584 (1984).
29. H. Totsuji, Phys. Rev. A 17, 399 (1978).
30. Yu. P. Monarkha, Fiz. Nizk. Temp. 3, 1459 (1977) [Sov.J.Low Phys.*3*, 702 (1977)].
31. V.B. Shikin, Zh.Eksp.Teor.Fiz. 60, 713 (1971) [Sov.Phys. JETP 33, 387 (1971)].
32. Yu. P. Monarkha, Fiz.Nizk.Temp. 1, 526 (1975) [Sov.J.Low Temp.Phys. 1, 258 (1975)].
33. G.A. Farias in PhD Thesis, IFQSC/USP (1980) unpublished. See also G.A. Farias, O. Hipólito and N. Studart, Proc. of 32 Annual Meeting of SBPC, Rio, Cienc.Cult.Supl. *32*(7), 260 (1980).
34. O. Hipólito, G.A. Farias and N. Studart, Surf. Sci. 113, 394 (1982).
35. S. Jackson and P.M. Platzman, Phys. Rev. B 24, 499 (1981) and Phys. Rev. B 25, 4886 (1982).
36. M. Saitoh, Surf. Sci. 142, 114 (1984) and references therein.
37. M. Degani and O. Hipólito, Surf. Sci. 142, 107 (1984).
38. E.L. Bodas and O. Hipólito, Phys. Rev. B 27, 6110 (1983).
39. M.H. Degani and O. Hipólito, Phys. Rev. B 32, 3300 (1985).
40. P. Leiderer, W. Ebner, V.B. Shikin, Surf.Sci.*113*, 405 (1982).
41. F.M. Peeters and P.M. Platzman, Phys. Rev. Lett. 50, 2021 (1983). See also F.M. Peeters, Phys. Rev. 30, 159 (1984).
42. M. Kosterlitz and D. Thouless, J. Phys. C 6, 1181 (1973).
43. B. Halperin and D. Nelson, Phys. Rev. B 19, 2457 (1979).
44. D.J. Thouless, J. Phys. C *11*, L189 (1978).
45. L.P. Gor'kov and D.M. Chernikova, Pis'ma Zh. Eksp.Teor.Fiz. *18*, 119

(1973) [JETP Lett. 18, 68 (1983)].

46. H. Etz, W. Gombert, W. Idstein and P. Leiderer, Phys. Rev. Lett.53, 2567 (1984).

47. U. de Freitas and N. Studart, II Workshop in Statistical Mechanics, dec. 1984, São Carlos (Brasil), unpublished.

Resumo

Resultados teóricos de algumas propriedades do sistema formado por elétrons bidimensionais sobre um filme de hélio líquido adsorvido em um substrato sólido são revistos neste trabalho. Descrevemos os estados superficiais eletrônicos tanto para elétrons sobre hélio volumétrico quanto para elétrons sobre filmes de hélio. Propriedades tais como o fator de estrutura e energia de correlação são determinadas em função da largura do filme para diferentes tipos de substrato através de uma Aproximação de Fases Aleatórias Generalizada. Descrevemos também as excitações coletivas deste sistema. Os resultados para elétrons sobre hélio volumétrico e filmes finos são facilmente obtidos. Examinamos a interação entre o elétron e as excitações da superfície do hélio líquido resultando na formação de um novo estado polarônico, que foi observado recentemente. A energia do estado fundamental e a massa efetiva deste polaron são determinadas pelo formalismo de integral de trajetória e método de transformação unitária. Discutimos ainda algumas especulações sobre o diagrama de fase dos elétrons sobre o filme de hélio.